Numerical study of double-diffusive natural convection in a square cavity

C. BÉGHEIN,† F. HAGHIGHAT‡ and F. ALLARD†

† Centre de Thermique de l'INSA de Lyon, URA CNRS 1372, INSA bât. 307,
F.69621 Villeurbanne Cedex, France
‡ Centre for Building Studies, Concordia University, Montreal, Quebec, Canada

Abstract—Steady-state thermosolutal convection in a square cavity filled with air, submitted to horizontal temperature and concentration gradients, is studied numerically. In the first series of numerical simulations, the influence of solutal buoyancy force on heat or mass transfer rate is investigated: Lewis and thermal Rayleigh numbers are kept constant ($Le = 1$, $Ra_T = 10^7$), solutal Rayleigh number is varied ($Ra_S = 10^5$ – 5×10^7). The second series deals with the influence of Lewis number on fluid motion for heat transfer driven flow ($Ra_T = 10^7$, $Ra_S = 0$) and mass transfer driven flow ($Ra_T = 0$, $Ra_S = 10^7$) configurations. Lewis number is varied from 0.3 to 5. Correlations are obtained between heat and mass transfer rates and the non-dimensional numbers characterizing both phenomena.

1. INTRODUCTION

DURING the past 30 years many experimental and numerical studies have been carried out concerning convective phenomena within cells. Most of these studies deal with fluid motion due only to temperature gradients. Nevertheless, fluid motion may be induced by density variations due to gradients of other scalar quantities. One of these quantities can be pollutant concentration within the fluid. Such a phenomenon, combining temperature and concentration buoyancy forces, is called double-diffusion.

Double-diffusion occurs in a very wide range of fields such as oceanography, astrophysics, geology, biology, chemical processes, etc. Ostrach [1] and Viskanta *et al.* [2] carried out a very complete state-of-the-art review. Ostrach focused his attention on the description of many types of flows (along flat plates, in plumes, in rectangular enclosures) while Viskanta *et al.* mostly studied fluid motions in thermohaline solutions.

Gebhart and Pera [3] were among the first ones to numerically study double-diffusion for cases of vertical laminar fluid motions along surfaces or in plumes. In this study, special attention was paid to the influence of non-dimensional parameters relevant to double-diffusion, on the heat and mass transport processes; transition to turbulence was mentioned. In 1985, Bejan [4] completed a fundamental study of scale analysis relative to heat and mass transport processes within cavities, submitted to horizontal temperature and concentration gradients. Pure thermal convection, pure solutal convection, heat transfer driven flows, and mass transfer driven flows were taken into account. Furthermore, in another report, Trevisan and Bejan [5] studied the boundary layer flow in the same configuration (under the stationary

regime) and varied several non-dimensional parameters: the Lewis and Prandtl numbers, and the buoyancy ratio. Lin *et al.* [6] repeated a similar study relative to the behaviour of the whole flow, under the unstationary regime. Other numerical works which are mainly concerned with chemical vapour deposition processes [7] dealt with very low Prandtl number (0.01) gases.

Experimental studies dealing with thermosolutal convection within rectangular cavities submitted to horizontal temperature and concentration gradients have been performed [8–10]. A layered flow structure was observed, according to particular values of the buoyancy ratio and of the Lewis number (very large), with both opposing or aiding buoyancy forces. The experimental results were in good agreement with Lee and Hyun's numerical results for double-diffusive convection in a rectangular cavity, under the unsteady state [11, 12].

This paper describes the results of a numerical study of steady-state double-diffusion in a square cavity filled with air ($Pr = 0.71$), submitted to either augmenting or opposing temperature and concentration buoyancy forces. The numerical procedure is based on the SIMPLER algorithm [13]. In the first part of the numerical study, the effect of location of the pollutant source on the hot or cold vertical walls, and of the positive or negative value of the concentration expansion coefficient on fluid motion, is studied. A parametric study of the influence of the strength of the concentration buoyancy force on fluid motion and on heat or mass transfer rates is carried out. The second part is devoted to the study of the effect of thermal and solutal diffusions on heat and mass transfer rates. The cavity is filled with air mixed with different kinds of pollutants which have a Lewis number range between 0.3 and 5. A qualitative study in the

NOMENCLATURE

C	non-dimensional concentration of pollutant	Sh_i	local Sherwood number (i-position along a vertical axis)
C^*	concentration of pollutant	T	non-dimensional temperature
C_∞	reference concentration	T^*	temperature
C_C, C_H	concentration of pollutant on the left and right vertical walls	T_∞	reference temperature of fluid mixture
D	mass diffusivity of pollutant through the fluid mixture	T_C, T_H	temperatures of the left and right vertical walls
g	gravitational acceleration	u_i, u, v	non-dimensional velocities (horizontal, vertical)
H	height of the enclosure	u_i^*	velocities
L	width of the enclosure	x_i, x, y	non-dimensional coordinates (horizontal, vertical)
Le	Lewis number, α/D	x_i^*	coordinates.
N	buoyancy ratio, $\beta_S \Delta C/(\beta_T \Delta T)$		
Nu	average Nusselt number (integrated over a vertical axis)		
Nu_i	local Nusselt number (i-position along a vertical axis)	**Greek symbols**	
P	non-dimensional pressure	α	thermal diffusivity
P^*	pressure	β_S	coefficient of volumetric expansion due to concentration change
Pr	Prandtl number, ν/α	β_T	coefficient of volumetric expansion due to temperature change
Ra_S	solutal Rayleigh number, $g\beta_S(C_H - C_C)H^3/(\nu D)$	δ_S	concentration boundary layer thickness
Ra_T	thermal Rayleigh number, $g\beta_T(T_H - T_C)H^3/(\nu\alpha)$	δ_T	thermal boundary layer thickness
Sh	average Sherwood number (integrated over a vertical axis)	ν	kinematic viscosity of fluid mixture
		ρ^*	density of fluid mixture
		ρ_∞	reference density of fluid mixture.

case of opposing flows helps to physically understand the influence of the Lewis number on fluid motion. A quantitative analysis enables us to quantify the average heat or mass transfer rates in the two limiting cases of heat transfer driven flows (high temperature gradients) and mass transfer driven flows (high concentration gradients).

2. PHYSICAL AND NUMERICAL MODELS

2.1. *Physical Model*

The physical model is a square, two-dimensional cavity, whose upper and lower horizontal walls are adiabatic and impermeable; the vertical ones are at different levels of temperature and concentration, in order to generate fluid motion (see Fig. 1).

The fluid contains a pollutant concentration. The pollutant and the fluid are completely mixed. Therefore, the system to be studied is the fluid mixture (fluid and pollutant).

2.2. *Model Equations*

The primitive variables of double-diffusion problems are the same ones as for pure convection problems (i.e. velocities, pressure, temperature), with an additional scalar quantity, which is the pollutant concentration of the fluid mixture. The behaviour of this quantity is globally similar to the temperature one.

As a result, the mathematical model of double-diffusion includes a concentration equation, obtained in the same way as the energy equation (mass balances in control volumes). Moreover, the buoyancy concentration force is taken into account by considering that for small density variations, the density of the fluid at constant pressure depends on the temperature and species concentration [14]

$$\rho^* \approx \rho_\infty + (\partial \rho^*/\partial T^*)_P(T^* - T_\infty)$$
$$+ (\partial \rho^*/\partial C^*)_P(C^* - C_\infty) + \cdots. \quad (1)$$

By analogy with the thermal processes, one can define a concentration expansion coefficient

$$\beta_S = -(1/\rho^*)(\partial \rho^*/\partial C^*)_P. \quad (2)$$

It is worth noting that the concentration expansion coefficient is slightly different from the thermal one: β_T (air or water) is always positive (an increase in temperature induces a decrease in density) while β_S may be either positive or negative (an increase in pollutant concentration, respectively, induces a decrease or an increase in density). These considerations lead to the Boussinesq approximation and to the vertical momentum equation.

The dimensionless variables of the stated problem are
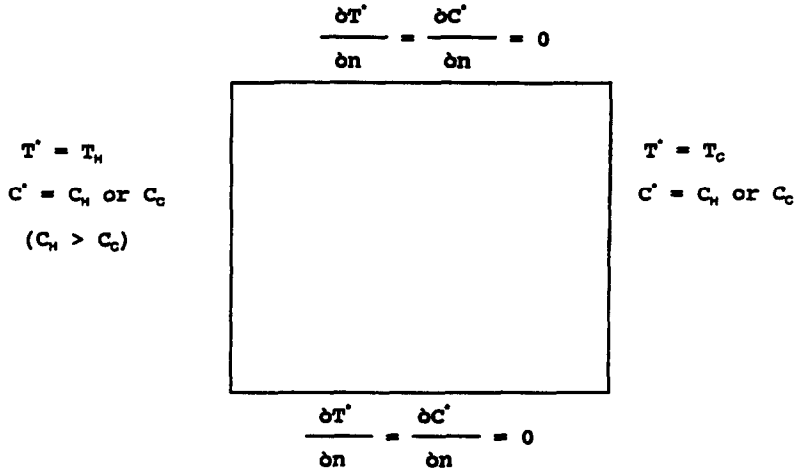
$$x_i = x_i^*/H \quad (3)$$

$$\frac{\partial T^*}{\partial n} = \frac{\partial C^*}{\partial n} = 0$$

$$T^* = T_H$$
$$C^* = C_H \text{ or } C_C$$
$$(C_H > C_C)$$

$$T^* = T_C$$
$$C^* = C_H \text{ or } C_C$$

$$\frac{\partial T^*}{\partial n} = \frac{\partial C^*}{\partial n} = 0$$

FIG. 1. Studied geometry.

$$u_i = u_i^* H/\alpha \tag{4}$$

$$T = \frac{T^* - T_C}{T_H - T_C} \tag{5}$$

$$C = \frac{C^* - C_C}{C_H - C_C} \tag{6}$$

$$P = P^* \rho^* \alpha^2 / H^2. \tag{7}$$

The reference temperature and concentration are $(T_H + T_C)/2$ and $(C_H + C_C)/2$, respectively.

With the above-mentioned dimensionless variables, the mathematical problems to be solved are:

continuity equation

$$\frac{\partial u_i}{\partial x_i} = 0; \tag{8}$$

momentum equation

$$u_j \frac{\partial u_i}{\partial x_j} - Pr \frac{\partial^2 u_i}{\partial x_j \partial x_j} = -\frac{\partial P}{\partial x_i} + Ra_T \, Pr(T-0.5)\delta_{i2}$$
$$+ Ra_S \frac{Pr}{Le}(C-0.5)\delta_{i2}; \tag{9}$$

energy equation

$$u_j \frac{\partial T}{\partial x_j} - \frac{\partial^2 T}{\partial x_j \partial x_j} = 0; \tag{10}$$

species diffusion equation

$$u_j \frac{\partial C}{\partial x_j} - \frac{1}{Le}\frac{\partial^2 C}{\partial x_j \partial x_j} = 0. \tag{11}$$

The boundary conditions of the stated problem are

$$u(0,y) = u(1,y) = u(x,0) = u(x,1) = 0 \tag{12}$$

$$v(0,y) = v(1,y) = v(x,0) = v(x,1) = 0 \tag{13}$$

$$T(0,y) = 1 \tag{14}$$

$$T(1,y) = 0 \tag{15}$$

$$C(0,y) = 1 \text{ or } 0 \tag{16}$$

$$C(1,y) = 0 \text{ or } 0 \tag{17}$$

$$\frac{\partial T(x,0)}{\partial x} = \frac{\partial T(x,1)}{\partial x} = \frac{\partial C(x,0)}{\partial x} = \frac{\partial C(x,1)}{\partial x} = 0. \tag{18}$$

2.3. Dimensionless Parameters

In equations (9) and (11), one must notice the presence of four dimensionless governing parameters:

thermal Rayleigh number

$$Ra_T = \frac{g\beta_T(T_H - T_C)H^3}{\nu\alpha}; \tag{19}$$

solutal Rayleigh number

$$Ra_S = \frac{g\beta_S(C_H - C_C)H^3}{\nu D}; \tag{20}$$

Prandtl number

$$Pr = \frac{\nu}{\alpha}; \tag{21}$$

Lewis number

$$Le = \frac{\alpha}{D}. \tag{22}$$

Each of these parameters influences the fluid motion.

Varying the values of thermal and solutal Rayleigh numbers modifies the buoyancy forces. Since the concentration expansion coefficient is negative or positive, and according to the location of the pollutant concentration on the hot or cold vertical walls, the solutal and thermal buoyancy forces may be either augmenting or opposing each other. In fact, four configurations of flows can be observed:
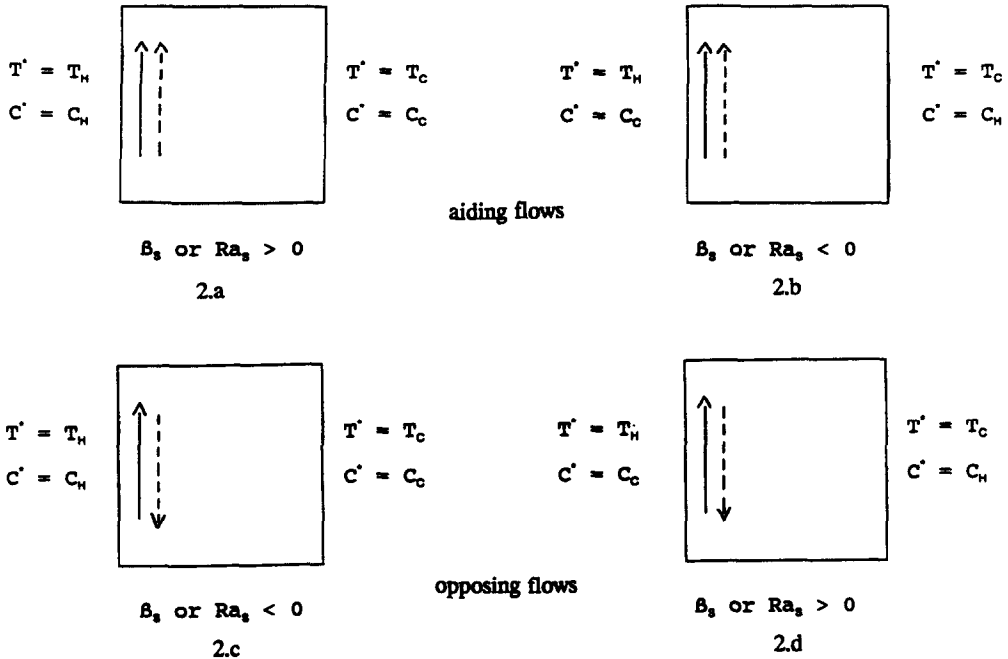
FIG. 2. Studied configurations ($C_H > C_C$, $T_H > T_C$): ----→, solutal buoyancy force; —→ thermal buoyancy force.

• two cases dealing with augmenting buoyancy forces (see Figs. 2(a) and (b));

• two cases dealing with opposing buoyancy forces (see Figs. 2(c) and (d)).

The Lewis number represents the ratio between the thermal and solutal diffusivities. It can also be expressed as a function of the Schmidt number (analogous to the Prandtl number)

$$Sc = \frac{v}{D}.$$ (23)

From both expressions of Prandtl and Schmidt numbers, one can write

$$Le = \frac{Sc}{Pr}.$$ (24)

For a Lewis number greater than unity, the solutal diffusivity is stronger than the thermal one; for a Lewis number less than unity, the thermal diffusivity is stronger than the solutal one. This will be studied in the second part of our numerical analysis.

2.4. Heat and Mass Transfer Rates

The local Nusselt (heat transfer rate) and local Sherwood (mass transfer rate) numbers on the *i*-position along a vertical axis are evaluated from the following expressions (using previously mentioned dimensionless variables):

$$Nu_i = u_i T - \frac{\partial T}{\partial x_i}$$ (25)

$$Sh_i = Le\left(u_i C - \frac{1}{Le}\frac{\partial C}{\partial x_i}\right).$$ (26)

The use of these expressions enable us to obtain conservative heat and mass transfer rates within the cavity [15, 16]. They include diffused and transported quantities which are integrated over the vertical axis in order to calculate the average heat or mass transfer rates (*Nu* or *Sh*) along this axis.

2.5. Numerical Procedure

The numerical resolution is the SIMPLER (Semi Implicit Method for Pressure Linked Equation Revised); developed by Patankar [13]. The model equations are spatially discretized over a staggered grid using the finite difference method and then integrated over control volumes. The SIMPLER algorithm is an iterative scheme which consists of correcting velocities a priori estimated with the momentum equations. As the iterative process converges, the velocities will fit the pressure correction equations derived from the continuity equation. The pressure and pressure correction equations are solved with a direct method, while for the other equations (momentum, energy and concentration), a Tri-Diagonal Matrix Algorithm (TDMA) [17] is used. In order to improve the convergence of the iterative procedure, an under-relaxation of the equations is necessary. The convergence of the algorithm is reached when the residual of the momentum equations is less than 10^{-2}. The physical domain is discretized into a non-uniform

Tchebycheff grid [18], which ensures thin grid spacing close to the walls, and a coarser mesh system in the core region.

3. RESULTS AND DISCUSSION

3.1. Effect of Buoyancy Forces

The flows considered in this part are augmenting or opposing flows, with $Le = 1$ and $Pr = 0.7$ (air). A Lewis number of unity means that the diffusion of pollutant concentration is the same as diffusion of temperature. As a result, the isopleths of concentration and temperature are similar.

3.1.1. Comparison of pure thermal convection-aiding flows

This first study consists of comparing pure thermal convection with thermosolutal convection, in the case of augmenting flows (Fig. 2(a)). For pure thermal convection, the thermal Rayleigh number is 2×10^4, while a solutal Rayleigh number of 10^4 and a thermal Rayleigh number of 10^4 are used to simulate thermosolutal convection. The same results are obtained: isopleths of concentration (or temperature) (Fig. 3(b)) and Sherwood (or Nusselt) numbers (Tables 1 and 2) in the latter case are similar to isopleths of temperature (Fig. 3(a)) and Nusselt numbers in the former case. This is explained by the fact that the contribution of the thermal and solutal buoyancy forces aiding each other is the same as the thermal one occurring in pure thermal convection. As a result, the two aiding solutal and thermal buoyancy forces (identical thermal and solutal diffusivities) are to be likened to the thermal natural convection effect.

3.1.2. Comparison of aiding flows (cases 2(a) and (b))

In the following numerical study, the respective locations of thermal and solutal boundary conditions are varied. The previous thermosolutal convection configuration is compared with the case described in Fig. 2(b) (the pollutant concentration is located on the cold vertical wall of the cavity, $Ra_S = -Ra_T = -10^4$). This configuration leads to identical isopleths of temperature to the former ones (Fig. 3(c)). Nevertheless, although there seems to be a similarity between the concentration and temperature patterns, one must keep in mind that concentration and temperature boundary conditions are reversed. Hence, there is a complementarity between the temperature and concentration dimensionless values; Sherwood and Nusselt numbers are the same in absolute value, but of opposite signs (Sherwood number is negative).

3.1.3. Comparison of opposing flows (cases 2(c) and (d))

The same kind of comparison is led concerning opposing flows (Figs. 2(c) and (d)). Both temperature patterns are presented in Figs. 3(d) and (e). Since thermal and solutal buoyancy forces are opposite, the buoyancy effects are cancelled; convection disappears

and the mass and heat transfers are diffusion dominated.

3.1.4. Influence of the solutal Rayleigh number

The configuration of the last series of numerical simulations relative to the effect of buoyancy forces is described in Fig. 2(d). Solutal and thermal Rayleigh numbers are positive, but the boundary conditions are reversed. The thermal Rayleigh number is kept constant ($Ra_T = 10^7$), the solutal Rayleigh number is increased from 10^6 up to 5×10^7. From Figs. 4 and 5, one can notice a stagnant core region (except for pure diffusion); the flow is mostly driven by fluid motion within the boundary layers. In the case of pure mass or thermal diffusion, there is no vertical buoyancy force. Hence, the velocities are equal in absolute value and the fluid motion is circular (Fig. 5(e)). There is no boundary layer regime; the isopleths of concentration or temperature are parallel and vertical (Fig. 4(e)). The flow is driven by the net effect of the two buoyancy forces. When the solutal Rayleigh number is less than the thermal one, the convection is thermal dominated and the flow is clockwise (Figs. 4(a)–(d) and 5(a)–(d)). A solutal Rayleigh number greater than the thermal one induces a concentration dominated counterclockwise flow (Figs. 4(f), (g) and 5(f), (g)). When the net effect of thermal and solutal buoyancy forces is opposite, symmetrical cases (Figs. 4(b), 5(b), 4(f) and 5(f)) are to be noted. For each of these simulations, the evolution of the average Nusselt number along the hot vertical wall was plotted (Figs. 6(a) and (b)). A new dimensionless governing parameter is used, i.e. the buoyancy ratio N. This number is the ratio between the solutal and the thermal buoyancy forces

$$N = \frac{\beta_S \Delta C^*}{\beta_T \Delta T^*} \qquad (27)$$

where

$$\Delta C^* = C^*(\text{left wall}) - C^*(\text{right wall})$$

$$\Delta T^* = T^*(\text{left wall}) - T^*(\text{right wall}).$$

It can be either positive or negative, according to the values of the concentration expansion coefficient and the location of the pollutant source (on the hot or cold vertical wall). Figure 6(a) ($N \leqslant -1$) shows that, when the fluid motion is induced by the thermal buoyancy force, the transported energy increases with N, i.e. the net buoyancy force increases. Since the fluid motion is clockwise, the buoyancy force is maximum at the bottom of the hot wall, hence the heat transfer rate is maximum. The reversed phenomenon is to be highlighted, when $N \geqslant -1$ (a solutal vertical gradient induces the fluid motion (Fig. 6(b)). Under these conditions, there is a correlation between the average Nusselt number within the cavity and the global buoyancy force $Ra_T \times \text{abs}(1 + N)$ (Table 3). (In the case of $Le = 1$, $Ra_T \times \text{abs}(1 + N) = Ra_T + Ra_S$.) This
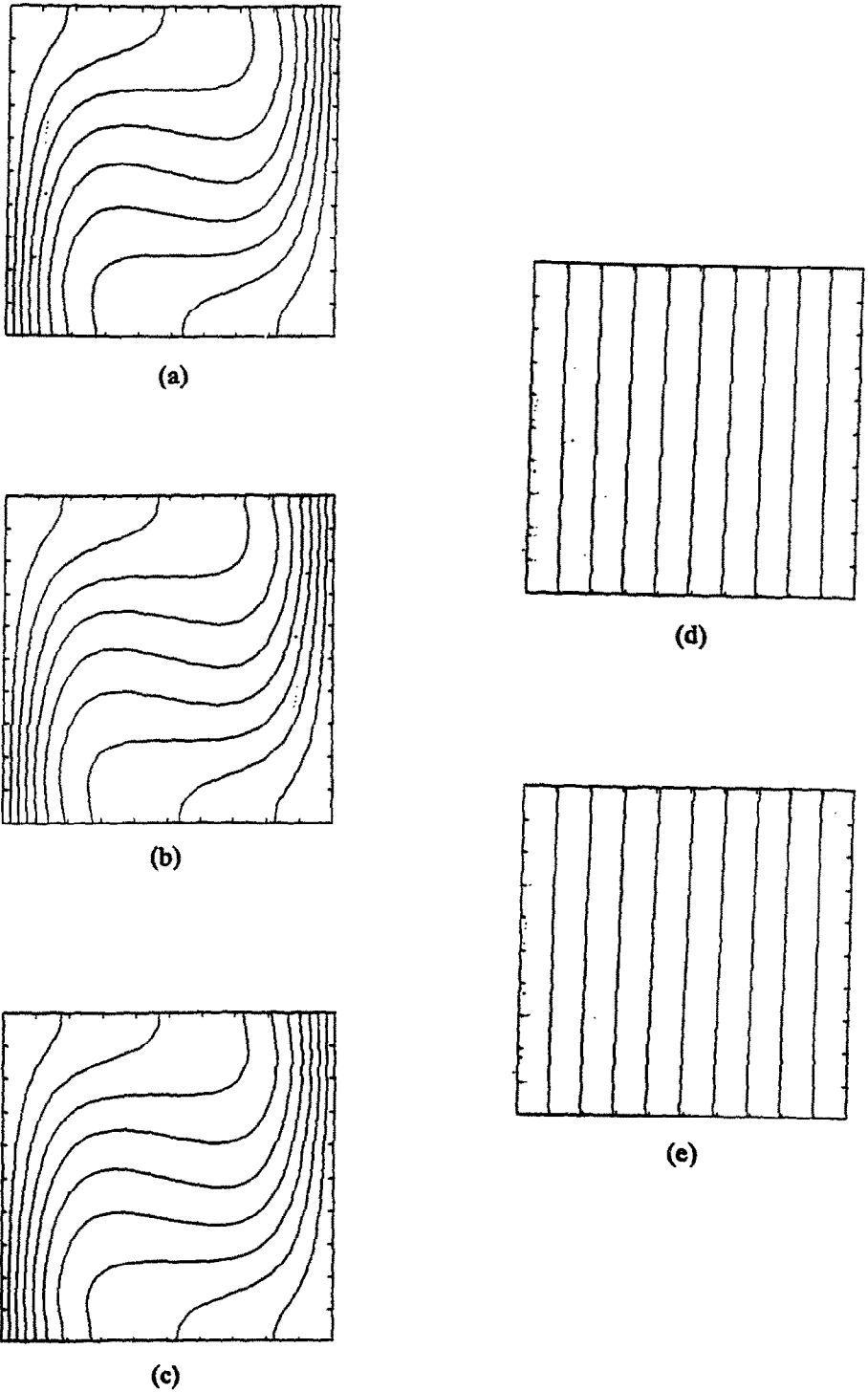
FIG. 3. Isopleths of temperature (pure thermal convection): (a) $Ra_T = 2 \times 10^4$. Isopleths of temperature (thermosolutal convection, $Le = 1$): (b) $Ra_T = 10^4$, $Ra_S = 10^4$, aiding flows; (c) $Ra_T = 10^4$, $Ra_S = 10^4$, aiding flows; (d) $Ra_T = 10^4$, $Ra_S = 10^4$, opposing flows; (e) $Ra_T = 10^4$, $Ra_S = -10^4$, opposing flows.

Table 1. Local Nusselt numbers along the left vertical wall, $Le = 1$, $Pr = 0.71$, $Ra_T = 10^4$

Dimensionless height	Local Nusselt number
0.001	4.16
0.009	4.17
0.022	4.20
0.039	4.25
0.062	4.32
0.089	4.39
0.120	4.42
0.155	4.42
0.193	4.36
0.235	4.25
0.279	4.09
0.326	3.89
0.374	3.65
0.424	3.39
0.475	3.11
0.525	2.82
0.576	2.52
0.626	2.23
0.674	1.93
0.721	1.65
0.765	1.39
0.807	1.16
0.845	0.97
0.880	0.83
0.911	0.74
0.938	0.68
0.961	0.65
0.978	0.64
0.991	0.63
0.999	0.63

Table 2. Local Nusselt and Sherwood numbers along the left vertical wall, $Le = 1$, $Pr = 0.71$, $Ra_T = Ra_S = 10^4$, aiding flows

Dimensionless height	Local Nusselt number	Local Sherwood number
0.001	4.18	4.18
0.009	4.18	4.18
0.022	4.21	4.21
0.039	4.26	4.26
0.062	4.33	4.33
0.089	4.39	4.39
0.120	4.43	4.43
0.155	4.42	4.42
0.193	4.36	4.36
0.235	4.25	4.25
0.279	4.09	4.09
0.326	3.89	3.89
0.374	3.65	3.65
0.424	3.39	3.39
0.475	3.11	3.11
0.525	2.82	2.82
0.576	2.52	2.52
0.626	2.22	2.22
0.674	1.93	1.93
0.721	1.65	1.65
0.765	1.39	1.39
0.807	1.16	1.16
0.845	0.97	0.97
0.880	0.83	0.83
0.911	0.74	0.74
0.938	0.68	0.68
0.961	0.66	0.66
0.978	0.64	0.64
0.991	0.64	0.64
0.999	0.64	0.64

relationship is illustrated in Fig. 7; the empirical correlation is given as follows:

$$Nu = 0.22(Ra_T \times abs\,(1+N))^{0.27}. \qquad (28)$$

The correlation coefficient is very good (0.9999). This relation seems to be in good agreement with the one developed by Trevisan and Bejan [5] for a cavity submitted to uniform heat and mass fluxes along the vertical sides. Moreover, the value of the exponent is very close to the boundary layer characteristic value relevant to natural convection in a cavity heated from the side [14].

3.2. Effect of the Lewis Number

The last series of numerical investigations studies the influence of the Lewis number on the heat and mass transfer processes within the cavity. The configuration to be studied is the one described in Fig. 2(d), dealing with opposing temperature and concentration horizontal gradients. The fluid filling the cavity is air ($Pr = 0.71$) mixed with different kinds of pollutant species. The Lewis numbers of pollutant mixed with air may vary between 0.2 and 5 ($25°C$ and 1 atm) [3]. The concentration expansion coefficient of the pollutant sources considered here is supposed to be positive. It should be noticed that these pollutant sources mixed with another fluid may have different characteristics: the concentration expansion coefficient of these species may be negative, and the Lewis

number of such constituents mixed with water is greater than 100.

The Lewis number deals with relative influence of thermal and mass diffusions. It has an effect on the thicknesses of the thermal and solutal boundary layers [4]. Grid refinement tests were performed in order to obtain grid independant results (35×35–45×45 Tchebycheff grids). Hence, both solutal and thermal boundary layers contain at least three grid points.

3.2.1. Qualitative study

Numerical results referring to the Lewis numbers varied from 0.5 up to 5 are given in Table 4 ($Ra_T = 10^7$, $Ra_S = 10^6$). Absolute values of Sherwood numbers along the hot vertical wall were drawn (Fig. 8). From this figure, two conclusions are to be registered:

• The Sherwood number increases with the Lewis number. This phenomenon is illustrated in relations (29)–(31) developed below (the type of flow studied here is a heat transfer driven flow: the thermal Rayleigh number is much higher than the solutal Rayleigh number).

• The Sherwood number is maximum at the bottom of the left hot wall, and it decreases from the bottom to the top of the wall. Since the thermal buoyancy force is stronger than the concentration one, the
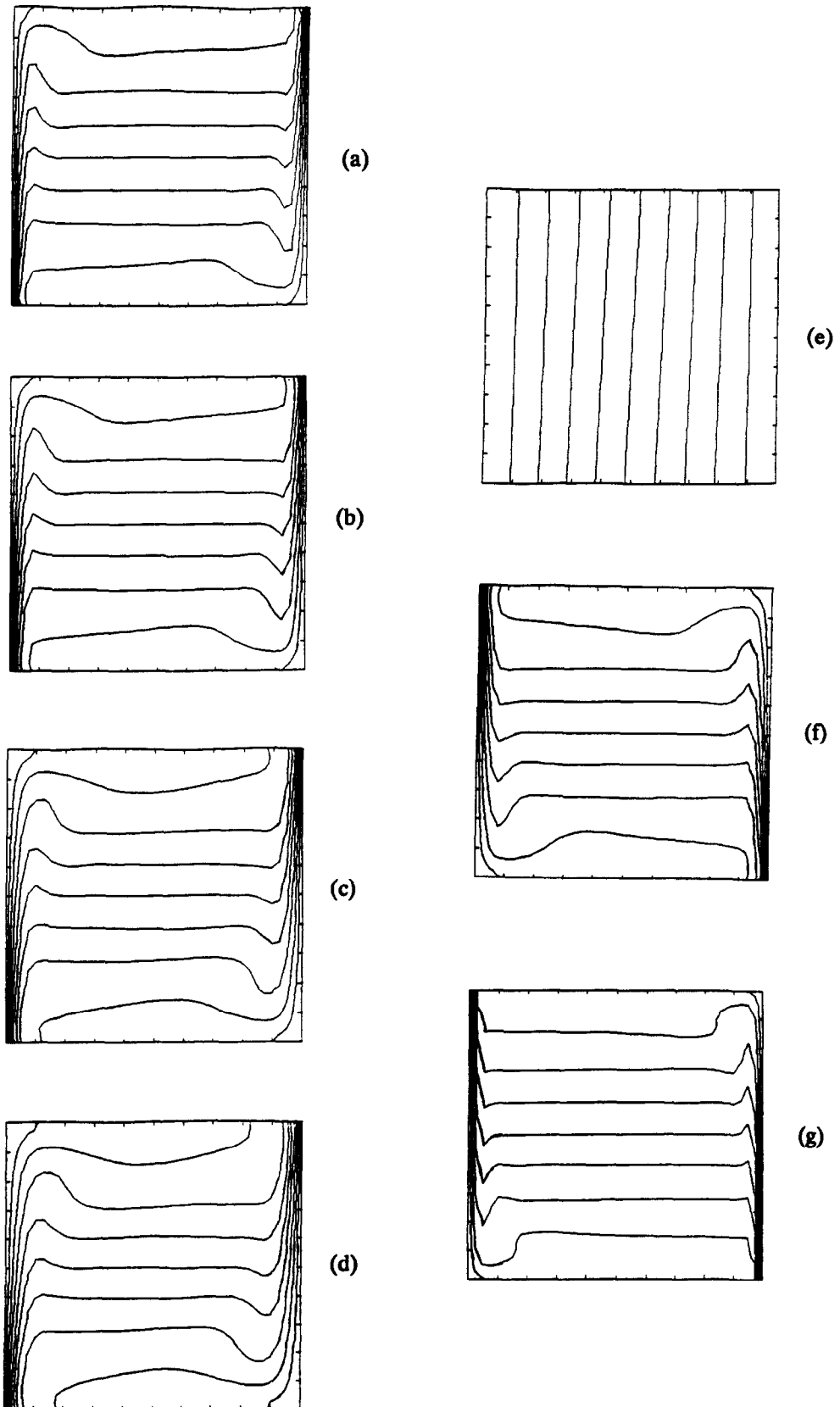
FIG. 4. Isopleths of temperature ($Le = 1$, $Ra_T = 10^7$, opposing flows): (a) $Ra_S = 10^6$; (b) $Ra_S = 5 \times 10^6$; (c) $Ra_S = 8 \times 10^6$; (d) $Ra_S = 9 \times 10^6$; (e) $Ra_S = 10^7$; (f) $Ra_S = 1.5 \times 10^7$; (g) $Ra_S = 5 \times 10^7$.
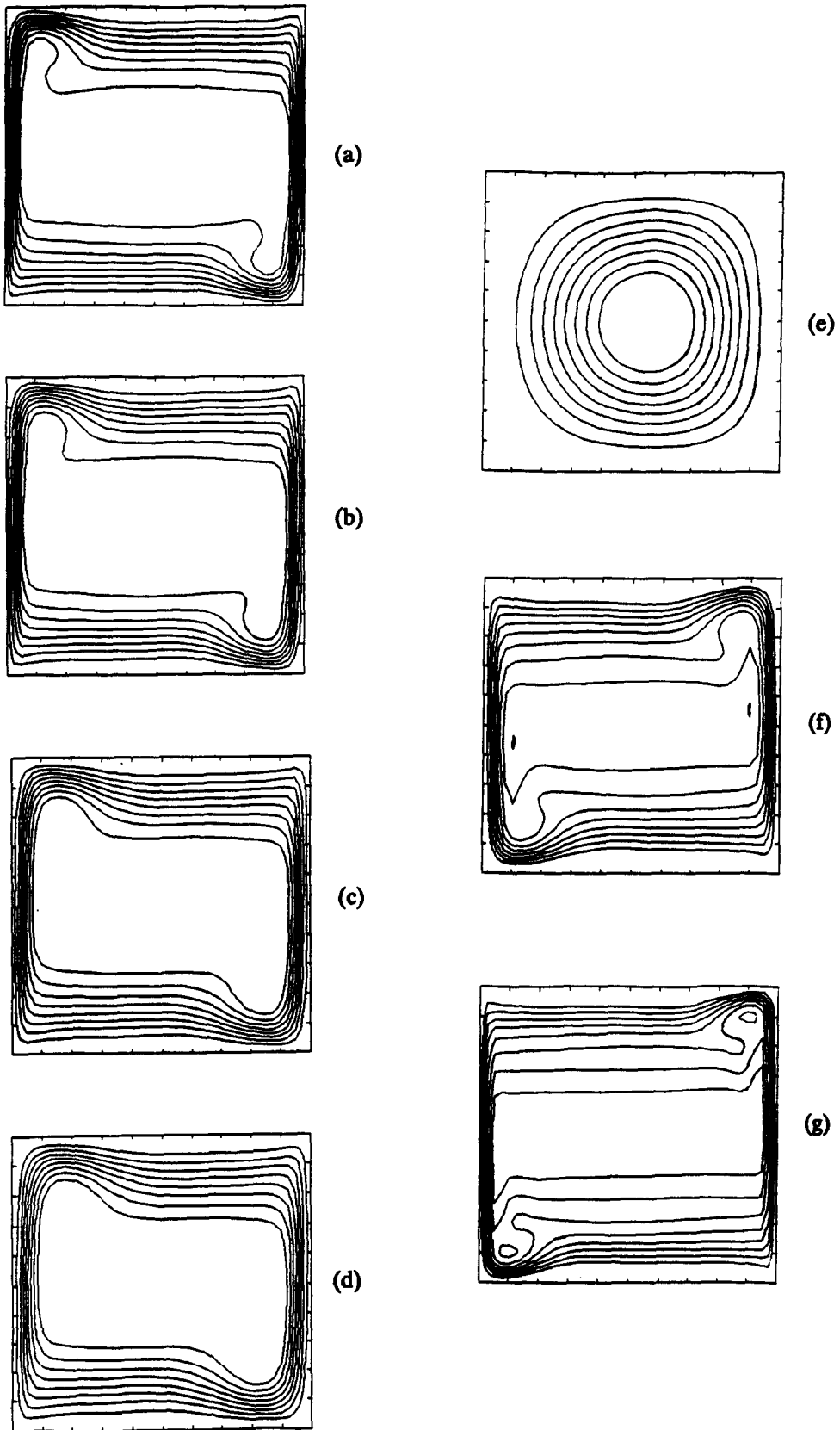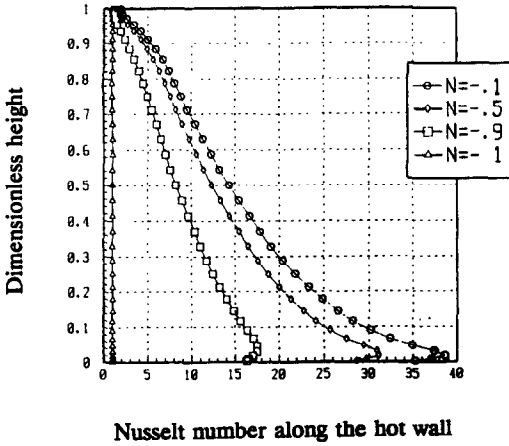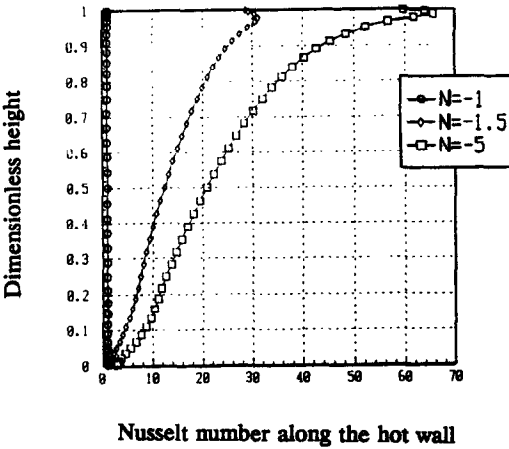
FIG. 5. Streamlines ($Le = 1$, $Ra_T = 10^7$, opposing flows): (a) $Ra_S = 10^6$; (b) $Ra_S = 5 \times 10^6$; (c) $Ra_S = 8 \times 10^6$; (d) $Ra_S = 9 \times 10^6$; (e) $Ra_S = 10^7$; (f) $Ra_S = 1.5 \times 10^7$; (g) $Ra_S = 5 \times 10^7$.

Nusselt number along the hot wall

(a)

Nusselt number along the hot wall

(b)

FIG. 6. Local Nusselt number along the hot wall, opposing flows, $Ra_T = 10^7$, $Le = 1$: (a) $N = -0.1$, -1; (b) $N = -1$, -5.

fluid motion is clockwise. The fluid near the bottom of the left wall is very polluted, and the concentration decreases as it moves along the left, non-polluted vertical wall; the velocity of the fluid mixture also decreases. Therefore, the Sherwood number along the left wall decreases.
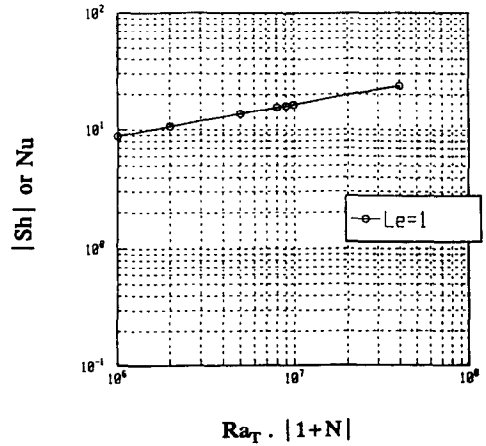
From isopleths of concentration (Fig. 9), it is to be

FIG. 7. Opposing flows, $Ra_T = 10^7$, $Le = 1$, $N = -0.01$, -5.

Table 4. Heat transfer driven flow, $Ra_T = 10^7$, $Pr = 0.71$, non-dimensional thermal boundary layer thickness, average Sherwood number

Le	Sc	δ_C/H	Sh
0.5	0.35	0.039	11.0
0.6	0.42	0.032	12.5
0.7	0.49	0.028	13.7
0.8	0.56	0.024	14.8
0.9	0.63	0.022	15.6
1.0	0.70	0.019	16.4
2.0	1.40	0.010	21.3
3.0	2.10	0.007	24.4
4.0	2.80	0.005	26.7
5.0	3.50	0.004	28.7

noticed that with Lewis numbers less than unity, the mass transfer process is diffusion dominated. The solutal boundary layer is rather thick, and the iso-concentration lines are tilted. The more the Lewis number is decreased, the more the isoconcentration lines are tilted, the more the pollutant concentration is diffused. The reverse phenomenon occurs when the Lewis number is greater than unity. The solutal boundary layer becomes thinner and thinner and the pollutant concentration less and less diffused. As the Lewis number is increased up to 5, the major mass transfer process is mass diffusion within the solutal boundary layer. The core region is filled with a homogeneous fluid. The massline pattern [5] (Fig. 10) in the case of $Le = 5$ reinforces this assertion.

Table 3. Average Nusselt and Sherwood numbers (along a vertical axis), $Le = 1$, $Pr = 0.71$, N is varied from -0.01 to -5

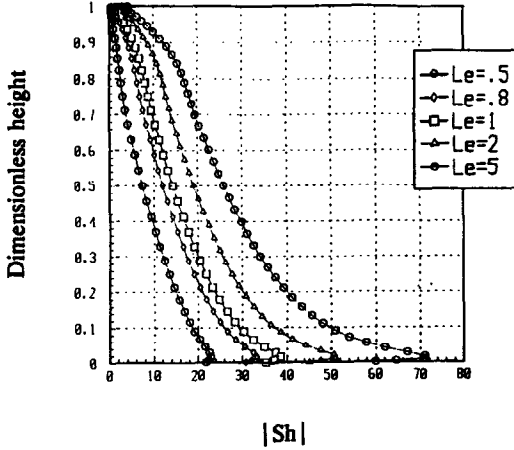|	$Ra_T = 10^7$							
					Ra_S			
	10^5	10^6	2×10^6	5×10^6	8×10^6	9×10^6	1.5×10^7	5×10^7
N	-0.01	-0.1	-0.2	-0.5	-0.8	-0.9	-1.5	-5.0
Nu	16.4	16.0	15.5	13.6	10.6	8.8	13.6	23.7
Sh	-16.4	-16.0	-15.5	-13.6	-10.6	-8.8	-13.6	-23.7

|Sh|

FIG. 8. Local Sherwood number along the hot wall, opposing flows, $Ra_T = 10^7$, $Ra_S = 10^6$, $Le = 0.5, 5$.

3.2.2. Quantitative study

Links were obtained between average Sherwood or Nusselt numbers and the characteristic numbers of double-diffusion, in the case described in Fig. 2(d). Two configurations were studied:

(a) heat transfer driven flows;
(b) mass transfer driven flows.

Heat (respectively mass) transfer driven flows are due to the temperature (respectively solutal) buoyancy force. Therefore, the solutal (respectively thermal) Rayleigh number is set to zero. This is an ideal case which helps acquire a better understanding of the influence of the characteristic numbers on the fluid motion.

3.2.2.1. *Heat transfer driven flows.* In order to obtain these links, we used the results of the scale analysis developed by Bejan (vertical flat plate) [4]. The scale analysis consists of evaluating the convection equations under the boundary layer regime. The length scales of the phenomena are the thermal, concentration and dynamic boundary layer thicknesses, and the height of the vertical plate. The boundary layer thicknesses are linked with the Prandtl, Schmidt and Lewis numbers. Therefore, several correlations are to be obtained according to these values. In the case of a Prandtl number less than unity, the following results are obtained (vertical flat plate):

$$Sc > 1 \qquad Sh \approx Le^{1/3} Pr^{1/12} Ra_T^{1/4} \qquad (29)$$

$$Sc < 1, Le > 1 \qquad Sh \approx Le^{1/2} Pr^{1/4} Ra_T^{1/4} \qquad (30)$$

$$Sc < 1, Le < 1 \qquad Sh \approx Le \, Pr^{1/4} Ra_T^{1/4}. \qquad (31)$$

To fit these equations on the mass transfer process in a cavity, one must make sure that the concentration boundary layer is smaller than the width of the cavity [4]. The aforementioned values of the average Sherwood number are obtained from the following expressions of the concentration boundary layer thickness ($Sh \approx H/\delta_C$):

$$Sc > 1 \qquad \delta_C/H \approx Le^{-1/3} Pr^{-1/12} Ra_T^{-1/4} \qquad (32)$$

$$Sc < 1, Le > 1 \qquad \delta_C/H \approx Le^{-1/2} Pr^{-1/4} Ra_T^{-1/4} \qquad (33)$$

$$Sc < 1, Le < 1 \qquad \delta_C/H \approx Le^{-1} Pr^{-1/4} Ra_T^{-}. \qquad (34)$$

The case to be studied here is a fluid ($Pr = 0.7$) mixed with different kinds of pollutant species ($Le = 0.3$–5); the thermal Rayleigh number is 10^7. The non-dimensional thickness of the concentration boundary layer is less than unity (Table 4). The average Sherwood numbers calculated from the numerical model are sketched in Table 4. From equations (29) and (31), one can check that the logarithmic value of the Sherwood number linearly depends on the logarithmic value of $Ra_T^{-1/4}$. Hence, we plotted the following relation:

$$\ln(Sh \, Ra_T^{-1/4}) = f(\ln(Le)) \qquad (35)$$

to illustrate equations (29) and (31) (Fig. 11). From Fig. 11, it can be pointed out that there seems to be a transition in the region $Le \approx 1$. The slope of the first part of the curve ($Le < 0.7$) is 0.8, while the slope of the second part ($Le > 2$) is 0.3. The second part of the curve seems to be in good agreement with the results of the scale analysis (equation (29)), while the first one does not (equation (31)). This discrepancy can be due to the very close Lewis numbers (0.3–0.7), but is mainly due to the configuration of the cavity itself. Applying this scale analysis to a tall cavity (with vertical sides which can be compared to a vertical flat plate) may induce more accurate results: the vertical velocity in a tall cavity of aspect ratio $L/H = 0.25$–0.5 tends to be identical to the one along a vertical flat plate; in the case of a square cavity, it is different [4].

3.2.2.2. *Mass transfer driven flows.* A similar series of numerical simulations were carried out in the case of mass transfer driven flows. The scale analysis relevant to the average Nusselt numbers gives the following results ($Pr < 1$):

$$Le > 1, Sc > 1 \qquad Nu \approx Le^{-1} Ra_S^{1/4} Sc^{1/2} \qquad (36)$$

$$Le < 1, Sc < 1 \qquad Nu \approx Le^{-1/2} Ra_S^{1/4} Sc^{1/4} \qquad (37)$$

$$Le > 1, Sc < 1 \qquad Nu \approx Le^{-1} Ra_S^{1/4} Sc^{1/4}. \qquad (38)$$

The thermal boundary layer thickness is calculated from

$$Le > 1, Sc > 1 \qquad \delta_T/H \approx Le \, Ra_S^{-1/4} Sc^{-1/2} \qquad (39)$$

$$Le < 1, Sc < 1 \qquad \delta_T/H \approx Le^{1/2} Ra_S^{-1/4} Sc^{-1/4} \qquad (40)$$

$$Le > 1, Sc < 1 \qquad \delta_T/H \approx Le \, Ra_S^{-1/4} Sc^{-1/4}. \qquad (41)$$

The input data and the results of the calculation (thermal boundary later thickness, average Nusselt number) are listed in Table 5. From equations (36) and (37), it can be pointed out that the logarithmic value of the Nusselt number linearly depends on the logarithmic value of $Ra_S^{1/4}$. Hence, the following relation was plotted in Fig. 12:
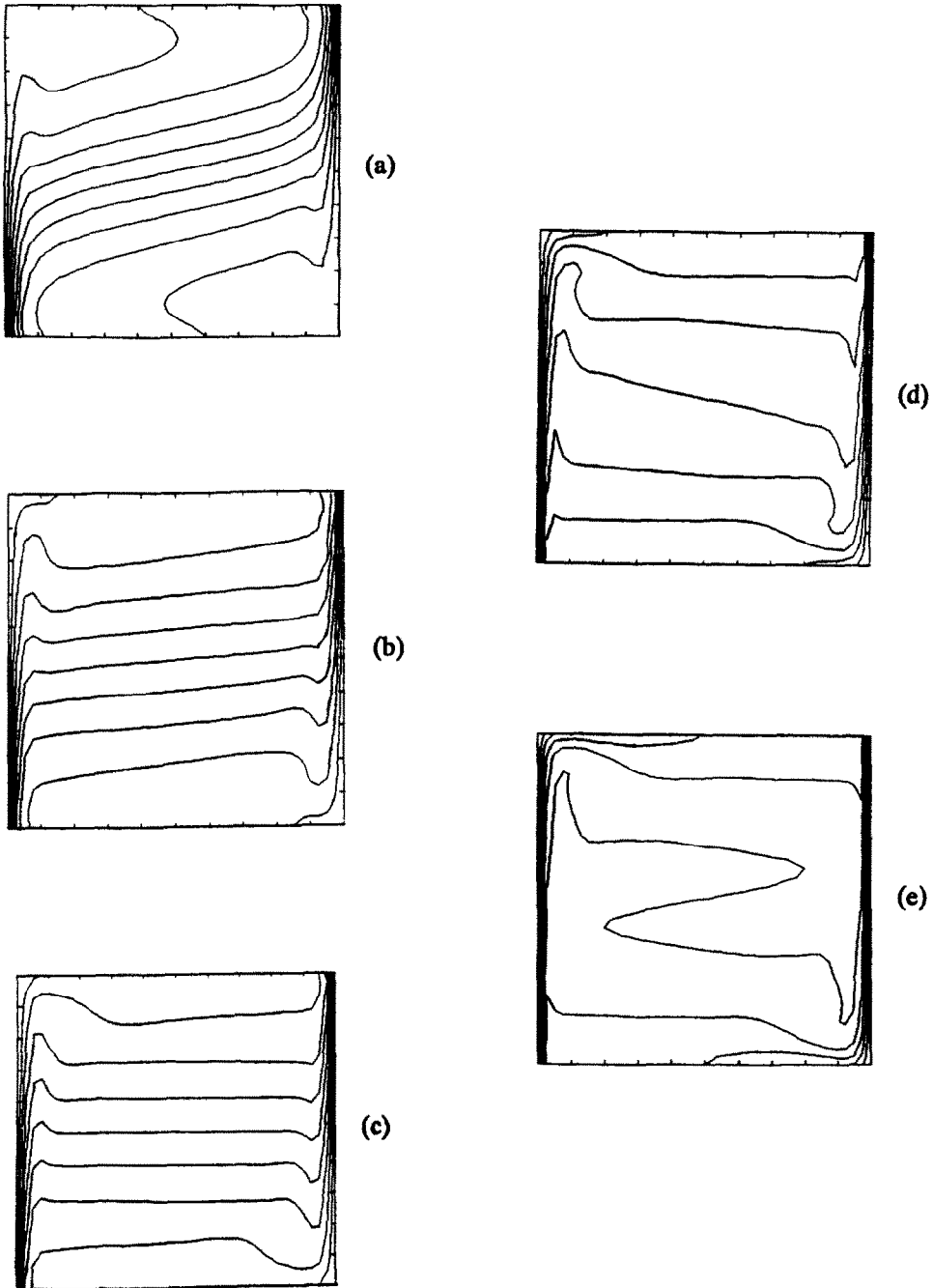
FIG. 9. Isopleths of concentration $(Ra_T = 10^7, Ra_S = 10^6$, opposing flows): (a) $Le = 0.5$; (b) $Le = 0.8$; (c) $Le = 1$; (d) $Le = 2$; (e) $Le = 5$.

$$\ln (Nu\, Ra_S^{-1/4}) = f(\ln (Le)). \qquad (42)$$

Similar results to the heat transfer driven flow ones are to be highlighted:

(a) transition in the $Le = 1$ region;
(b) linear dependence on the Lewis number:

$Le < 0.7$:   the slope of the curve is -0.3,

$Le < 1$:   the slope of the curve is -0.8.

4. CONCLUDING REMARKS

A numerical procedure based on the SIMPLER algorithm was used to investigate stationary thermo-solutal convection in a square cavity submitted to
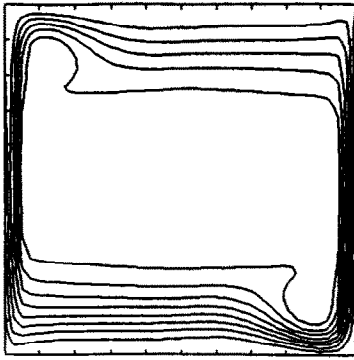
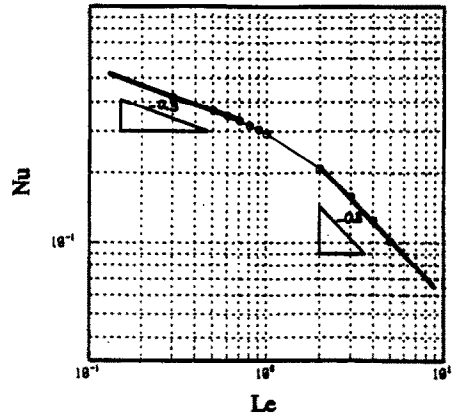FIG. 10. Mass lines, $Ra_T = 10^7$, $Ra_S = 10^6$, opposing flows, $Le = 5$.

FIG. 12. Mass transfer driven flow, average Nusselt number.

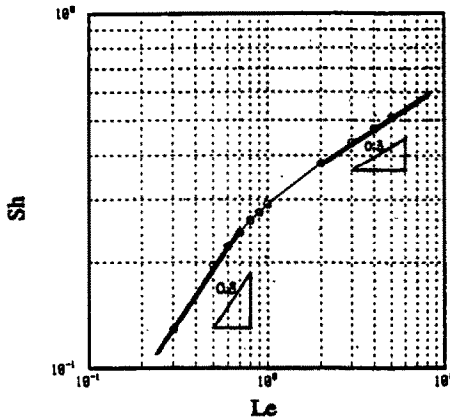

FIG. 11. Heat transfer driven flow, average Sherwood number.

Table 5. Mass transfer driven flow, $Ra_S = 10^7$, $Pr = 0.71$, non-dimensional thermal boundary layer thickness, average Nusselt number

Le	Sc	δ_T/H	Nu
0.5	0.35	0.36	20.5
0.6	0.42	0.35	19.5
0.7	0.49	0.33	18.6
0.8	0.56	0.32	17.8
0.9	0.63	0.30	17.1
1.0	0.70	0.29	16.4
2.0	1.40	0.21	11.7
3.0	2.10	0.16	8.8
4.0	2.80	0.12	7.0
5.0	3.50	0.10	5.7

augmenting or opposing thermal and solutal gradients. The cavity is filled with air mixed with different kinds of pollutants. A series of numerical experiments was performed, dealing with thermosolutal convection relevant to pollutants with the Lewis number as unity. The thermal buoyancy force is kept constant whilst the solutal buoyancy force is varied. According to the value of the solutal buoyancy force (i.e. solutal

Rayleigh number) and to the location of the pollutant source, the fluid motion may be either clockwise or counterclockwise; the combined effects of thermal and solutal buoyancy forces are to be compared with the effect of one thermal or solutal dominated buoyancy force, in the case of $Le = 1$. A correlation relevant to Nusselt or Sherwood numbers was obtained. In the latter series of numerical experiments, the Lewis number is varied from 0.3 to 5, in the case of opposing buoyancy forces. When the Lewis number is less than unity, the concentration boundary layer is rather thick; hence, the cavity is filled with a high diffusion pollutant, the isopleths of concentration are tilted. When the Lewis number is much greater than unity, the solutal boundary layer is thinner, the pollutant is diffused within the concentration boundary layer, therefore the core of the cavity is filled with a homogeneous fluid. Wall heat and mass transfer rates are quantitatively estimated from correlations in the cases of heat transfer driven flows and mass transfer driven flows. These correlations, which show a dependence of heat and mass transfer rates on Lewis number, are in agreement with the plane vertical plate results.

REFERENCES

1. S. Ostrach, Natural convection with combined driving forces, *PhysicoChem. Hydrodyn.* **1**, 233–247 (1980).
2. R. Viskanta, T. L. Bergman and F. P. Incropera, Double-diffusive natural convection. In *Natural Convection: Fundamentals and Applications* (Edited by S. Kakac, W. Aung and R. Viskanta), pp. 1075–1099. Hemisphere, Washington, DC (1985).
3. B. Gebhart and L. Pera, The nature of vertical natural convection flows resulting from the combined buoyancy effects of thermal and mass diffusion, *Int. J. Heat Mass Transfer* **14**, 2025–2050 (1971).

4. A. Bejan, Mass and heat transfer by natural convection in a vertical cavity, *Int. J. Heat Fluid Flow* **6**, 149–159 (1985).

5. O. V. Trevisan and A. Bejan, Combined heat and mass transfer by natural convection in a vertical enclosure, *ASME J. Heat Transfer* **109**, 104–112 (1987).

6. T. F. Lin, C. C. Huang and T. S. Chang, Transient binary mixture natural convection in square enclosures, *Int. J. Heat Mass Transfer* **33**, 287–299 (1990).

7. P. Ranganathan and R. Viskanta, Natural convection of a binary gas in rectangular cavities. *ASME-JSME Thermal Engng Joint Conf.*, Hawaii (1987).

8. Y. Kamotani, L. W. Wang, S. Ostrach and H. D. Jiang, Experimental study of natural convection in shallow enclosures with horizontal temperature and concentration gradients, *Int. J. Heat Mass Transfer* **28**, 165–173 (1985).

9. S. Ostrach, H. D. Jiang and Y. Kamotani, Thermosolutal convection in shallow enclosures, *ASME-JSME Thermal Engng Joint Conf.*, Hawaii (1987).

10. J. Lee, M. T. Hyun and K. W. Kim, Natural convection in confined fluids with combined horizontal temperature and concentration gradients, *Int. J. Heat Mass Transfer* **31**, 1969–1977 (1988).

11. J. M. Hyun and J. W. Lee, Double-diffusive convection in a rectangle with cooperating horizontal gradients of

12. J. W. Lee and J. M. Hyun, Double-diffusive convection in a rectangle with opposing horizontal and concentration gradients, *Int. J. Heat Mass Transfer* **33**, 1619–1632 (1990).

13. S. V. Patankar, *Numerical Heat Transfer and Fluid Flow*. McGraw-Hill, London (1980).

14. A. Bejan, *Convection Heat Transfer*. Wiley, New York (1984).

15. F. Allard, Contribution à l'étude des transferts de chaleur dans les cavités thermiquement entrainees—application aux cellules d'habitation, Thèse de doctorat d'état, Institut National des Sciences Appliquées de Lyon, Lyon I, 336 pp. (1987).

16. J. P. Simoneau, Etude de l'interaction entre un jet et la convection naturelle dans une cellule d'habitation, Thèse de doctorat, Institut National des Sciences Appliquées de Lyon, Lyon I, 243 pp. (1989).

17. D. A. Anderson, J. C. Tannehill and R. H. Pletcher, *Computational Fluid Mechanics and Heat Transfer*. Hemisphere, Washington, DC (1983).

18. P. Haldenwang, Resolution tridimensionnelle des équations de Navier–Stokes par méthodes spectrales Tchebycheff, Thèse d'état, Université de Provence, Marseille (1984).

temperature and concentration gradients, *Int. J. Heat Mass Transfer* **33**, 1605–1617 (1990).

ETUDE NUMERIQUE DE LA DOUBLE DIFFUSION DANS UNE CAVITE CARREE

Résumé—La convection thermosolutale, en régime stationnaire, dans une cavité carrée remplie d'air, soumise à des gradients horizontaux de température et de concentration, est étudiée numériquement. Dans la première série de simulations, on étudie l'influence de la force de poussée solutale sur les taux de transfert de chaleur ou de masse : les nombres de Lewis et de Rayleigh thermique sont constants ($Le = 1$, $Ra_T = 10^7$), le nombre de Rayleigh solutal varie ($Ra_S = 10^5$ à 5×10^7). La deuxième série de simulations se rapporte à l'analyse de l'influence du nombre de Lewis sur le mouvement du fluide, dans les cas d'écoulements à force de poussée thermique dominante ($Ra_T = 10^7$, $Ra_S = 0$) et à force de poussée solutale dominante ($Ra_T = 0$, $Ra_S = 10^7$). Le nombre de Lewis varie de 0.3 à 5. Des corrélations sont obtenues entre les taux de transfert de chaleur et de masse et les nombres adimensionnels caractérisant les deux phénomènes.

NUMERISCHE UNTERSUCHUNG DER DOPPELT-DIFFUSIVEN NATÜRLICHEN KONVEKTION IN EINEM QUADRATISCHEN HOHLRAUM

Zusammenfassung—Es wird die stationäre doppelt-diffusive Konvektion in einem quadratischen luftgefüllten Hohlraum unter dem Einfluß horizontaler Temperatur- und Konzentrations-Gradienten numerisch untersucht. Eine erste Reihe numerischer Simulationen befaßt sich mit dem Einfluß der konzentrationsbedingten Auftriebskraft auf den Wärme- oder Stoffübergang: Die Lewis- und die thermische Rayleigh-Zahl werden konstant gehalten ($Le = 1$; $Ra_T = 10^7$), die Konzentrations-Rayleigh-Zahl wird im Bereich $10^5 \leqslant Ra_S \leqslant 5 \times 10^7$ variiert. Eine zweite Reihe behandelt den Einfluß der Lewis-Zahl auf die Fluidbewegung für thermisch getriebene ($Ra_T = 10^7$; $Ra_S = 0$) und konzentrationsgetriebene Anordnungen ($Ra_T = 0$; $Ra_S = 10^7$). Die Lewis-Zahl wird dabei im Bereich 0,3–5 variiert. Es ergeben sich Korrelationen zwischen den Wärme- und Stoffübergangskoeffizienten sowie für die dimensionslosen Kennzahlen, welche beide Phänomene charakterisieren.

ЧИСЛЕННОЕ ИССЛЕДОВАНИЕ ЕСТЕСТВЕННОЙ КОНВЕКЦИИ В КВАДРАТНОЙ ПОЛОСТИ

Аннотация—Численно исследуется стационарный перенос тепла и массы в заполненной воздухом квадратной полости при наложении градиентов температур и концентраций в горизонтальном направлении. В первой серии численных расчетов исследуется влияние подъемной силы за счет растворенного вещества на скорость тепло- и массопереноса. При этом число Льюиса и тепловое число Рэлея сохраняются постоянными ($Le = I$, $Ra_T = 10^7$), число Рэлея для растворенного вещества изменяется ($Ra_S = 10^5$–5×10^7). Во второй серии расчетов устанавливается влияние числа Льюиса на движение жидкости для течений за счет теплопереноса ($Ra_T = 10^7$, $Ra_S = 0$) и массопереноса ($Ra_T = 0$, $Ra_S = 10^7$). Число Льюиса варьируется от 0,3 до 5. Получены обобщающие соотношения для скоростей тепло- и массопереноса, выражаемых через безразмерные критерии, характеризующие эти явления.